Unfractionated heparin attenuates endothelial barrier dysfunction via the phosphatidylinositol-3 kinase/serine/threonine kinase/nuclear factor kappa-B pathway

Sheng-Tian Mu[1], Jie Tang[1], Jian-Qi Ma[1], Yu Zhong[1], Han-Zhe Liu[1], Xiao-Chun Ma[2], Zhen Zheng[1]

[1]Department of Intensive Care Unit, Cancer Hospital of China Medical University, Liaoning Cancer Hospital and Institute, Shenyang, Liaoning 110042, China; [2]Department of Intensive Care Unit, The First Affiliated Hospital of China Medical University, Shenyang, Liaoning 110001, China.

Abstract

Background: Vascular endothelial dysfunction is considered a key pathophysiologic process for the development of acute lung injury. In this study, we aimed at investigating the effects of unfractionated heparin (UFH) on the lipopolysaccharide (LPS)-induced changes of vascular endothelial-cadherin (VE-cadherin) and the potential underlying mechanisms.

Methods: Male C57BL/6 J mice were randomized into three groups: vehicle, LPS, and LPS + UFH groups. Intraperitoneal injection of 30 mg/kg LPS was used to induce sepsis. Mice in the LPS + UFH group received subcutaneous injection of 8 U UFH 0.5 h before LPS injection. The lung tissue of the mice was collected for assessing lung injury by measuring the lung wet/dry (W/D) weight ratio and observing histological changes. Human pulmonary microvascular endothelial cells (HPMECs) were cultured and used to analyze the effects of UFH on LPS- or tumor necrosis factor-alpha (TNF-α)-induced vascular hyperpermeability, membrane expression of VE-cadherin, p120-catenin, and phosphorylated myosin light chain (p-MLC), and F-actin remodeling, and on the LPS-induced activation of the phosphatidylinositol-3 kinase (PI3K)/serine/threonine kinase (Akt)/nuclear factor kappa-B (NF-κB) signaling pathway.

Results: *In vivo*, UFH pretreatment significantly attenuated LPS-induced pulmonary histopathological changes (neutrophil infiltration and erythrocyte effusion, alveolus pulmonis collapse, and thicker septum), decreased the lung W/D, and increased protein concentration (LPS *vs.* LPS + UFH: 0.57 ± 0.04 *vs.* 0.32 ± 0.04 mg/mL, $P = 0.0092$), total cell count (LPS *vs.* LPS + UFH: 9.57 ± 1.23 *vs.* $3.65 \pm 0.78 \times 10^5$/mL, $P = 0.0155$), polymorphonuclear neutrophil percentage (LPS *vs.* LPS + UFH: $88.05\% \pm 2.88\%$ *vs.* $22.20\% \pm 3.92\%$, $P = 0.0002$), and TNF-α (460.33 ± 23.48 *vs.* 189.33 ± 14.19 pg/mL, $P = 0.0006$) in the bronchoalveolar lavage fluid. *In vitro*, UFH pre-treatment prevented the LPS-induced decrease in the membrane expression of VE-cadherin (LPS *vs.* LPS + UFH: 0.368 ± 0.044 *vs.* 0.716 ± 0.064, $P = 0.0114$) and p120-catenin (LPS *vs.* LPS + UFH: 0.208 ± 0.018 *vs.* 0.924 ± 0.092, $P = 0.0016$), and the LPS-induced increase in the expression of p-MLC (LPS *vs.* LPS + UFH: 0.972 ± 0.092 *vs.* 0.293 ± 0.025, $P = 0.0021$). Furthermore, UFH attenuated LPS- and TNF-α-induced hyperpermeability of HPMECs (LPS *vs.* LPS + UFH: 8.90 ± 0.66 *vs.* 15.84 ± 1.09 Ω·cm^2, $P = 0.0056$; TNF-α *vs.* TNF-α + UFH: 11.28 ± 0.64 *vs.* 18.15 ± 0.98 Ω·cm^2, $P = 0.0042$) and F-actin remodeling (LPS *vs.* LPS + UFH: 56.25 ± 1.51 *vs.* 39.70 ± 1.98, $P = 0.0027$; TNF-α *vs.* TNF-α + UFH: 55.42 ± 1.42 *vs.* 36.51 ± 1.20, $P = 0.0005$) *in vitro*. Additionally, UFH decreased the phosphorylation of Akt (LPS *vs.* LPS + UFH: 0.977 ± 0.081 *vs.* 0.466 ± 0.035, $P = 0.0045$) and I kappa B Kinase (IKK) (LPS *vs.* LPS + UFH: 1.023 ± 0.070 *vs.* 0.578 ± 0.044, $P = 0.0060$), and the nuclear translocation of NF-κB (LPS *vs.* LPS + UFH: 1.003 ± 0.077 *vs.* 0.503 ± 0.065, $P = 0.0078$) in HPMECs, which was similar to the effect of the PI3K inhibitor, wortmannin.

Conclusions: The protective effect of UFH against LPS-induced pulmonary endothelial barrier dysfunction involves VE-cadherin stabilization and PI3K/Akt/NF-κB signaling.

Keywords: Acute lung injury; Cadherin; Capillary permeability; Heparin

Introduction

Acute lung injury (ALI), leading to an excessive inflammatory response in the lungs, is a critical disease with a high incidence. It is associated with high morbidity and mortality due to its acute and serious symptoms. Despite extensive research and an increasing understanding of the pathogenesis of ALI, effective therapies are limited. Currently, research on ALI focuses on endothelial permeability as pulmonary edema caused by endothelial barrier destruction is the marker of the disease, yielding promising results.[1,2]

Access this article online

Quick Response Code:

Website: www.cmj.org

DOI: 10.1097/CM9.0000000000000905

Correspondence to: Zhen Zheng, Department of Intensive Care Unit, Cancer Hospital of China Medical University, Liaoning Cancer Hospital and Institute, No. 44 Xiaoheyan Road, Shenyang, Liaoning 110042, China
E-Mail: zhengzhen_lncan@126.com

Chinese Medical Journal 2020;133(15)

Received: 21-04-2020 **Edited by:** Qiang Shi

Vascular endothelial cadherin (VE-cadherin)-based adherens junctions are important players in regulating vascular permeability.[3,4] A previous study showed that intravenous injection of anti-VE-cadherin antibodies into mice substantially increased vascular permeability and fragility, leading to hemorrhage.[5] Lipopolysaccharide (LPS) from gram-negative bacteria stimulates the production of a variety of proinflammatory cytokines, which cause endothelial hyperpermeability by disrupting VE-cadherin-mediated cell-cell junctions.[6,7] VE-cadherin is recruited to the adherens junctions where it makes a physical link with the actin cytoskeleton. In vascular endothelial cells, it has been reported that, forces between VE-cadherin and the actin cytoskeleton may prevent leukocyte exosmosis and vascular permeability *in vivo* by stabilizing VE-cadherin mediated cell-cell junctions.[8] p120-catenin bound to the cytoplasmic tail of VE-cadherin is directly involved in stabilizing cadherin expression at the cell membrane. Studies showed that dissociation of p120-catenin from the cadherin complex leads to VE-cadherin endocytosis.[9-11]

Unfractionated heparin (UFH), a common anticoagulant agent, has been reported to suppress vascular permeability and improve endothelial barrier functions[12]; however, the exact mechanism is not clear. Our previous studies have demonstrated that LPS-induced endothelial barrier dysfunction was improved by UFH by preventing actin cytoskeleton remodeling and microtubule stabilization *in vitro* and *in vivo*.[13-15] However, the possibility that the ability of UFH to ameliorate LPS-induced endothelial barrier dysfunction is related to the expression of VE-cadherin and p120-catenin remains unexplored.

The phosphatidylinositol-3 kinase/serine/threonine kinase (PI3K/Akt) signaling pathway is involved in multiple biological processes, including cell-cell junction formation and cell proliferation and migration. Recently, the PI3K/Akt signaling pathway was identified as indispensable for the regulation of various cellular and molecular responses to endothelial barrier injury.[16-18] Nuclear factor kappa-B (NF-κB) is involved in inflammation and endothelial damage by activating different signal cascades, especially in response to PI3K/Akt signaling.[19,20] We previously demonstrated that the PI3K-IKK-IκB signaling pathway is involved in the regulation of tumor necrosis factor-alpha (TNF-α)-induced inducible nitric oxide synthase (iNOS) levels *in vitro*.[21] We have also shown that UFH attenuates interleukin-8 (IL-8) secretion via the PI3K/Akt/NF-κB signaling pathway.[22] However, it is still unknown whether PI3K/Akt/NF-κB signaling is involved in the VE-cadherin- and p120-catenin-based endothelial barrier dysfunction in ALI. Herein, we investigated whether the PI3K/Akt/NF-κB pathway is related to the UFH-mediated improvement of VE-cadherin and p120-catenin changes induced by LPS and endothelial barrier dysfunction.

Methods

Animal studies

All experimental procedures involving animals were handled according to the guidelines of the Experimental Animal Administration Committee of China Medical University. Research protocols were approved by the Experimental Animal Ethics Committee of China Medical University. Male C57BL/6 mice, weighing 20 to 25 g, were provided by the Laboratory Animal Center of China Medical University and randomly assigned to three groups, namely, vehicle group, LPS group, and LPS + UFH group. Sterile saline solution (LPS group) or UFH (8 U, subcutaneous injection, LPS + UFH group) was injected 30 min before intraperitoneal LPS administration (30 mg/kg) (Sigma, MO, USA).[23] Six hours after LPS administration, the mice were sacrificed under anesthesia and lung tissue samples were collected for further experiments.[13,15] As previously described, lung injury was assessed by measuring the lung wet/dry (W/D) weight ratio and observing histological changes.[13]

Bronchoalveolar lavage

The mice were lavaged with 1 mL phosphate buffered saline (PBS), intraperitoneally injected, under anesthesia, and the bronchoalveolar lavage fluid (BALF) was obtained. After centrifugation at $300 \times g$ for 10 min at 4°C, the supernatant was obtained and preserved at −80°C for TNF-α and total protein analyses. The total protein concentration in BALF was detected with a commercial bicinchoninic acid (BCA) assay kit following the manufacturer's instructions (Beyotime, Shanghai, China). The TNF-α levels were measured by an enzyme-linked immunosorbent assay (Nanjing KeyGen Biotech. Co., Ltd., Nanjing, China). The sediment was treated with erythrocyte lysate (Beyotime) for 10 min, and then centrifuged at $300 \times g$ for 10 min at 4°C. Subsequently, the cells were resuspended in 500 μL PBS and observed using an inverted microscope (Leica DMi8, Leica Microsystems, Germany).

Cells and cell treatment

Human pulmonary microvascular endothelial cells (HPMECs) obtained from ScienCell Research Laboratories (Carlsbad, CA, USA) were cultured in Dulbecco modified Eagle medium supplemented with 10% fetal bovine serum (Invitrogen, USA) in a CO_2 incubator at 37°C, with an atmosphere of 5% CO_2/95% air.[15] HPMECs of passage number 4 to 8 were used for all experiments.

Measurement of transendothelial permeability

Changes of the transendothelial electrical resistance (TEER) of endothelial cells were measured with the Millicell-ERS (MERS00002, Millipore, Bedford, MA, USA). An *in vitro* transendothelial permeability assay was performed quantifying transendothelial passage of fluorescein isothiocyanate-dextran (FITC-dextran, 40-kDa; Sigma). HPMECs were seeded at a density of 1.5×10^5cells/well on 24-well Transwell plates (Greiner Bio-One, pore size: 0.4 mm; diameter: 6.5 mm, Costar, The Netherlands), and were stimulated with 10 μg/mL of LPS or 10 ng/mL of TNF-α (R&D Systems, Abingdon, UK). After stimulation for 1, 6, 12, and 24 h, the TEER across the HPMECs was measured. To evaluate the effect of UFH on HPMEC hyperpermeability induced by LPS or TNF-α, the cells were stimulated by 10 μg/mL of LPS or 10 ng/mL

of TNF-α for 6 h after pre-treatment with vehicle or UFH (10 U/mL). The measurements were performed as previously described.[24]

Immunofluorescence and image analysis

HPMECs cultured on coverslips, untreated or pre-treated with UFH (10 U/mL) or PI3K inhibitor, wortmannin (100 nmol/L; Calbiochem, San Diego, CA, USA) for 30 min, were exposed to 10 μg/mL of LPS or 10 ng/mL of TNF-α for 6 h. Then, the cells were fixed with 4% paraformaldehyde for 0.5 h, permeabilized with 0.1% Triton X-100 for 5 min, and washed with PBS. After blocking with 5% bovine serum albumin (BSA) for 1 h, the coverslips were incubated with rabbit anti-VE-cadherin (1:200; Abcam, San Francisco, CA, USA) or rabbit anti-p120-catenin (1:200, Abcam) primary antibodies overnight at 4°C, followed by three washes with PBS for 5 min each. Then, the coverslips were incubated with a donkey anti-rabbit Alexa Fluor® 488 secondary antibody (Abcam) for 1 h at 37°C. Tetramethylrhodamine isothiocyanate-phalloidin was used to stain the actin cytoskeleton, while the HPMEC nuclei were counterstained with 4,6-diamino-2-phenyl indole (blue). Immunofluorescence images were acquired with a microscope (Leica DMi8, Leica Microsystems) equipped with a 40× objective. The Image J software (National Institute of Health, Bethesda, MD, USA) was used to define cell borders and calculate the vacant area in the images.[15]

Western blot analysis

HPMECs, untreated or pre-treated with 10 U/mL of UFH or 100 nmol/L wortmannin for 30 min, were stimulated with 10 μg/mL of LPS for 6 h and lysed with radioimmunoprecipitation assay lysis buffer (KeyGEN Biotech Co., Ltd.) to extract total protein. For membrane protein extraction, the membrane protein extraction kit (KeyGen Biotech) was used. Nuclear proteins were extracted with the nuclear protein extraction kit (Beyotime) following the manufacturer's instructions.[21] All extracted proteins were quantified using a BCA kit and were separated by sodium dodecyl sulfate-polyacrylamide gel electrophoresis on a 12% gel (20 μg protein/lane), followed by trans-blotting onto polyvinylidene fluoride membranes (Millipore). After blocking with 5% BSA, the membranes were incubated overnight at 4°C with primary antibodies against phospho-Akt (1:1000; Cell Signaling Technology), Akt (1:1000; Cell Signaling Technology), phospho-IKK (1:1000; Cell Signaling Technology), IKK (1:1000; Cell Signaling Technology), IκB (1:1000; Santa Cruz, CA, USA), VE-cadherin (1:1000), p120-catenin (1:2000), phosphorylated myosin light chain (p-MLC) (1: 1000; Cell Signaling Technology), MLC (1:1000; Cell Signaling Technology), Na^+/K^+-ATPase (1:1000; Beyotime), or β-actin (1:1000) to detect total or membrane proteins, or with primary antibodies against NF-κB (1:1000; Santa Cruz) and histone H3 (1:1000; Cell Signaling Technology) to detect nuclear proteins. Subsequently, the membranes were washed with Tris-buffered saline Tween-20 (TBST) three times for 10 min each, followed by incubation with horseradish peroxidase-conjugated goat anti-rabbit IgG (Bio-Rad). After washing with TBST three times for 10 min each, enhanced chemiluminescence was measured using the Plus kit (Amersham, Sweden) and quantified using the Image J software (National Institutes for Health, Bethesda, MD, USA). Na^+/K^+-ATPase, β-actin, and histone H3 served as loading controls. Each experiment was repeated three times.

Statistical analysis

The GraphPad Prism 6.0 software (La Jolla, CA, USA) was used for data analysis. Data are represented as means ± standard deviations. Differences between the groups were evaluated by the Student's *t* test. A value of $P < 0.05$ was considered to denote statistical significance.

Results

UFH counteracts LPS-induced endothelial barrier dysfunction by preventing inflammation and increasing VE-cadherin membrane expression in vivo

Hematoxylin and eosin staining was performed to observe histopathologic changes in the lung. Compared with the vehicle group, the lungs of mice in the LPS group displayed neutrophil infiltration and erythrocyte effusion, alveolus pulmonis collapse, and thicker septum. However, theses histopathologic changes were ameliorated by the administration of UFH [Figure 1A]. Furthermore, the protein content, total cell counts, and percentage of polymorphonuclear neutrophils (PMN) in BALF were analyzed to evaluate the extent of lung injury. The results show that LPS stimulation markedly enhanced protein content (0.57 ± 0.04 *vs.* 0.16 ± 0.02 mg/mL, $P = 0.0006$), total cell counts (9.57 ± 1.23 *vs.* $1.09 \pm 0.19 \times 10^5$/mL, $P = 0.0025$), and the percentage of PMN ($88.05\% \pm 2.88\%$ *vs.* $7.45\% \pm 1.85\%$, $P < 0.0001$) when compared with the vehicle group. However, comparison between the LPS and LPS + UFH groups showed that UFH significantly decreased protein concentration (0.57 ± 0.04 *vs.* 0.32 ± 0.04 mg/mL, $P = 0.0092$), total cell count (9.57 ± 1.23 *vs.* $3.65 \pm 0.78 \times 10^5$/mL, $P = 0.0155$), and PMN percentage ($88.05\% \pm 2.88\%$ *vs.* $22.20\% \pm 3.92\%$, $P = 0.0002$) [Figure 1B].

In order to assess lung edema, the lung W/D ratio was measured. As shown in Figure 1C, the LPS group showed higher lung W/D ratio than the control group (6.93 ± 0.20 *vs.* 3.97 ± 0.26, $P = 0.0009$). However, UFH pre-treatment ameliorated the LPS-stimulated lung edema (LPS + UFH *vs.* LPS: 5.05 ± 0.18 *vs.* 6.93 ± 0.20, $P = 0.0022$). Additionally, quantification of TNF-α production in BALF showed markedly higher TNF-α levels in the LPS group than in the vehicle group (460.33 ± 23.48 *vs.* 189.33 ± 14.19 pg/mL, $P = 0.0006$). However, administration of UFH decreased the levels of TNF-α production (LPS *vs.* LPS + UFH: 460.33 ± 23.48 *vs.* 189.33 ± 14.19 pg/mL, $P = 0.0006$) in BALF [Figure 1D].

To further explore the effects of UFH on the vascular barrier function, formation of adhesion junctions was assessed by quantifying the expression of VE-cadherin and p-120 catenin by Western blot analysis. The results show that LPS stimulation decreased the membrane expression of VE-cadherin and p-120 catenin. UFH was able to reverse this LPS-induced decrease of VE-cadherin and p-120 catenin expression [Figure 1E].

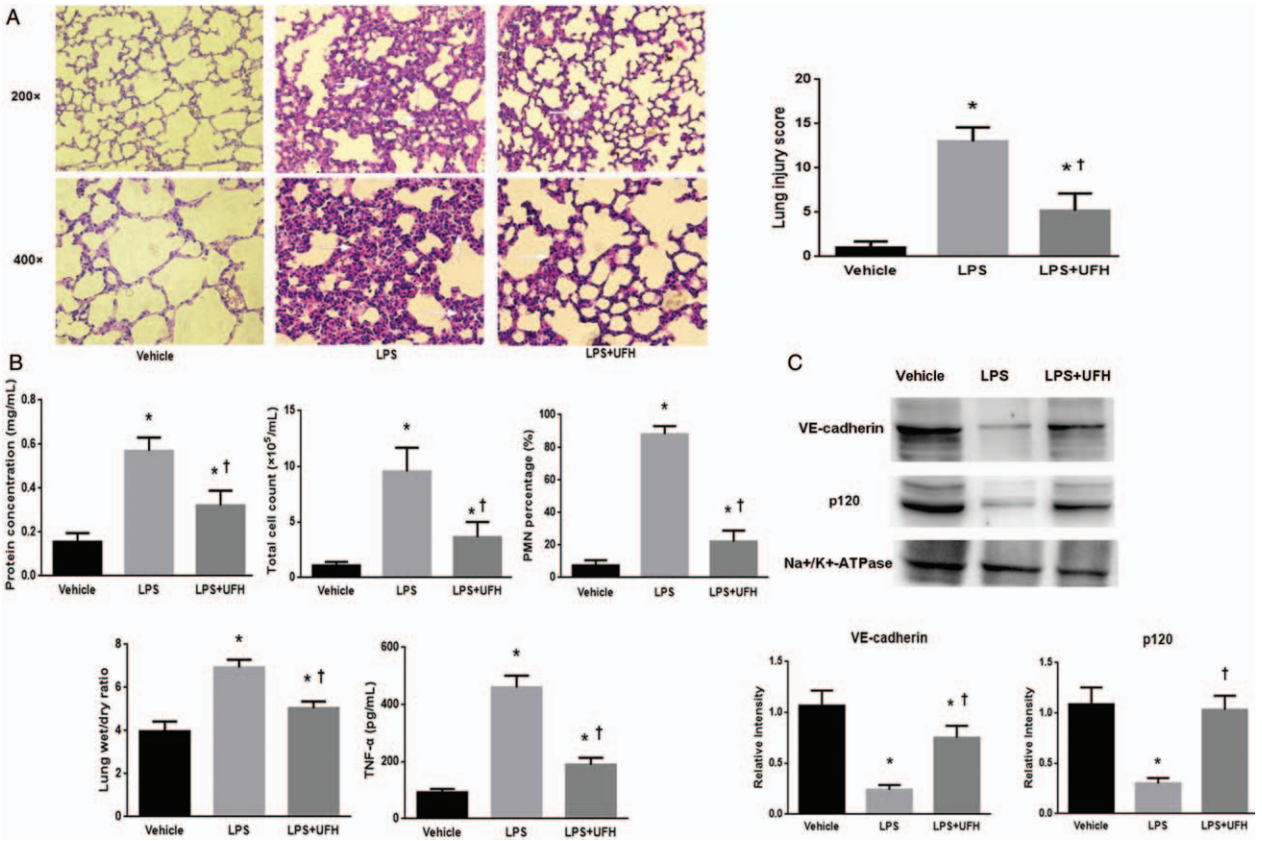

Figure 1: Effect of UFH on LPS-induced inflammation and endothelial barrier dysfunction *in vivo*. C57BL/6 mice were challenged with LPS (30 mg/kg, intraperitoneally) for 6 h with or without subcutaneous injection of UFH (8 U). (A) HE staining (original magnification, ×200 and ×400, respectively). Pre-treatment with UFH inhibited the LPS-induced pulmonary histopathological changes. White arrows indicate lung lesions. (B) Protein concentration, total cell count, PMN percentage, lung weight/dry ratio, and TNF-α levels after treatment. Data are expressed as mean ± standard deviation ($n = 3$ in each group); $^{*}P < 0.05$, compared with vehicle, $^{\dagger}P < 0.05$, compared with LPS treatment. (C) Western blot analysis. UFH significantly ameliorated the LPS-stimulated decrease in the membrane protein expression of VE-cadherin and p-120 catenin *in vivo*. Data are presented as mean ± standard deviation ($n = 3$ in each group). $^{*}P < 0.05$, compared with vehicle. $^{\dagger}P < 0.05$, compared with LPS alone. BAL: Bronchoalveolar lavage; LPS: Lipopolysaccharide; PMN: Polymorphonuclear neutrophils; TNF-α: Tumor necrosis factor-α; UFH: Unfractionated heparin; VE-cadherin: Vascular endothelial-cadherin.

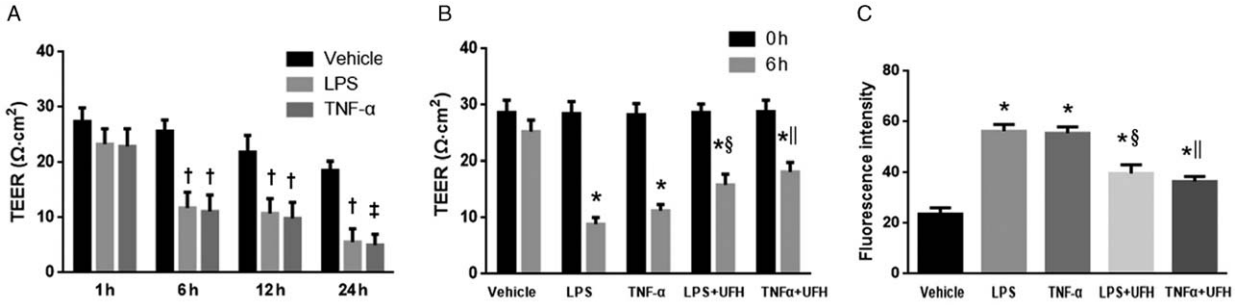

Figure 2: Effect of UFH pre-treatment on LPS- or TNF-α-induced increase in endothelial cell permeability. (A) The permeability of endothelial cells was assessed by measuring TEER across the cells at 1, 6, 12, and 24 h after stimulation with LPS (10 μg/mL) or TNF-α (10 ng/mL). (B and C) The TEER and the influx of fluorescein isothiocyanate-conjugated dextran across the cells. HPMECs were pre-treated with vehicle or UFH, followed by LPS or TNF-α challenge for 6 h. Data are representative of three independent experiments. $^{*}P < 0.05$ compared with the vehicle group, $^{\dagger}P < 0.01$ compared with the vehicle group, $^{\ddagger}P < 0.001$ compared with the vehicle group; $^{\S}P < 0.05$ compared with the LPS group, $^{\|}P < 0.05$ compared with the TNF-α group. HPMECs: Human pulmonary microvascular endothelial cells; LPS: Lipopolysaccharide; TEER: Transendothelial electrical resistance; TNF-α: Tumor necrosis factor-α; UFH: unfractionated heparin.

UFH attenuates LPS- or TNF-α-induced HPMEC hyperpermeability

To study the endothelial barrier function, the TEER of HPMECs was measured. We found that hyperpermeability of HPMECs could be induced by 10 μg/mL of LPS or 10 ng/mL of TNF-α, with the monolayer TEER decreasing with increasing stimulation time, especially after stimulation for more than 6 h [Figure 2A]. Therefore, 6 h stimulation of HPMEC with 10 μg/mL of LPS or 10 ng/mL of TNF-α was used for further experiments.

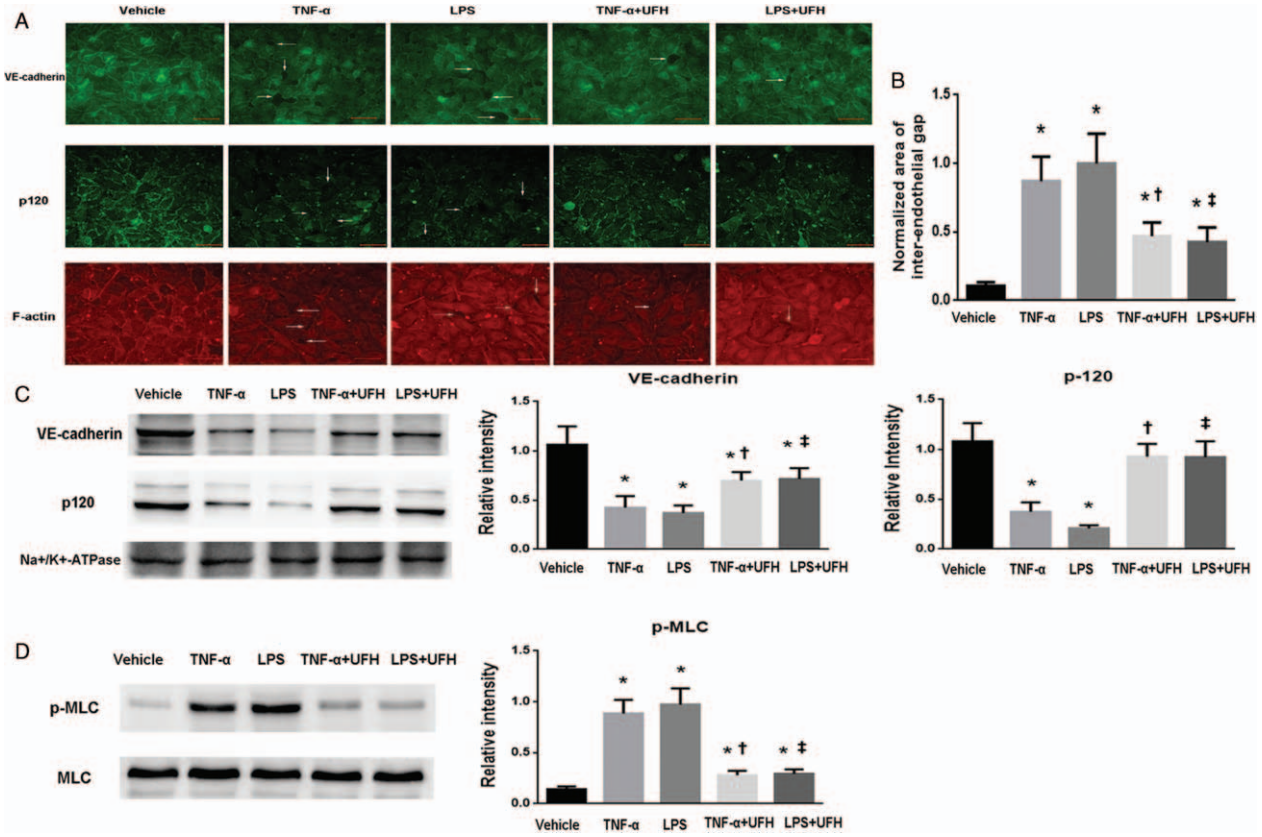

Figure 3: Effect of UFH pre-treatment on LPS- or TNF-α-induced decrease in VE-cadherin membrane expression and F-actin remodeling in HPMECs. (A) Immunofluorescence staining for VE-cadherin and p120-catenin, and tetramethylrhodamine isothiocyanate-phalloidin staining for F-actin. Arrows indicate intercellular gaps. Scale bar = 50 μm. (B) Area of inter-endothelial gaps. The gap area in the field of view was assessed and normalized to the gap area induced with LPS alone. For each group, a total of nine fields of view from three parallel experiments were analyzed. (C) Western blot analysis was used to evaluate the membrane expression of VE-cadherin and p120-catenin. Equal protein loading was confirmed by the Na^+/K^+-ATPase signal. (D) Western blot analysis was used to evaluate p-MLC expression. Equal protein loading was confirmed by the total MLC signal. Data are representative of three independent experiments. $^*P < 0.05$ compared with the vehicle group, $^\dagger P < 0.05$ compared with the LPS-treated group, $^\ddagger P < 0.05$ compared with the TNF-α group. HPMECs: Human pulmonary microvascular endothelial cells; LPS: Lipopolysaccharide; MLC: Myosin light chain; TNF-α: Tumor necrosis factor-α; TRITC: Tetramethylrhodamine isothiocyanate; UFH: Unfractionated heparin; VE-cadherin: Vascular endothelial-cadherin.

To evaluate the effect of UFH on the permeability of the HPMEC monolayer, TEER and the flux of FITC-labeled dextran were measured. As expected, UFH treatment increased TEER (LPS *vs.* LPS + UFH: 8.90 ± 0.66 *vs.* 15.84 ± 1.09 $\Omega \cdot cm^2$, $P = 0.0056$; TNF-α *vs.* TNF-α + UFH: 11.28 ± 0.64 *vs.* 18.15 ± 0.98 $\Omega \cdot cm^2$, $P = 0.0042$) and decreased the flux of FITC-labeled dextran (LPS *vs.* LPS + UFH, 56.25 ± 1.51 *vs.* 39.70 ± 1.98, $P = 0.0027$; TNF-α *vs.* TNF-α + UFH, 55.42 ± 1.42 *vs.* 36.51 ± 1.20, $P = 0.0005$), suggesting that UFH prevented HPMECs hyperpermeability induced by LPS or TNF-α [Figure 2B and 2C].

UFH ameliorates the LPS- or TNF-α-induced decrease in membrane expression of VE-cadherin and p120-catenin, increase in p-MLC expression, and F-actin remodeling in HPMECs

To assess how UFH affected the LPS- or TNF-α-induced changes in VE-cadherin and p120-catenin expression, immunofluorescence staining and Western blot analysis were performed. In the vehicle group, VE-cadherin and p120-catenin were predominantly localized in the cell periphery and paracellular gap. Compared with the vehicle group, LPS or TNF-α stimulation decreased the membrane localization of VE-cadherin and p120-catenin, causing paracellular gap formation. UFH prevented such LPS- or TNF-α-induced changes in the membrane localization of VE-cadherin (LPS *vs.* LPS + UFH: 0.368 ± 0.044 *vs.* 0.716 ± 0.064, $P = 0.0114$; TNF-α *vs.* TNF-α + UFH: 0.424 ± 0.067 *vs.* 0.701 ± 0.049, $P = 0.0301$) and p120-catenin (LPS *vs.* LPS + UFH: 0.208 ± 0.018 *vs.* 0.924 ± 0.092, $P = 0.0016$; TNF-α *vs.* TNF-α + UFH: 0.376 ± 0.054 *vs.* 0.930 ± 0.074, $P = 0.0038$) [Figure 3A–C]. Furthermore, UFH also ameliorated LPS- or TNF-α-induced F-actin remodeling, and stress fiber and paracellular gap formation, as indicated by phalloidin immunofluorescence staining. Additionally, UFH prevented the increase of p-MLC expression (LPS *vs.* LPS + UFH: 0.972 ± 0.092 *vs.* 0.293 ± 0.025, $P = 0.0021$; TNF-α *vs.* TNF-α + UFH, 0.885 ± 0.077 *vs.* 0.280 ± 0.025, $P = 0.0017$) induced by LPS or TNF-α [Figure 3D].

Taken together, our observations suggest that UFH reinforces the barrier of HPMECs by stabilizing VE-cadherin and p120-catenin, decreasing p-MLC, and preventing reorganization of the actin cytoskeleton.

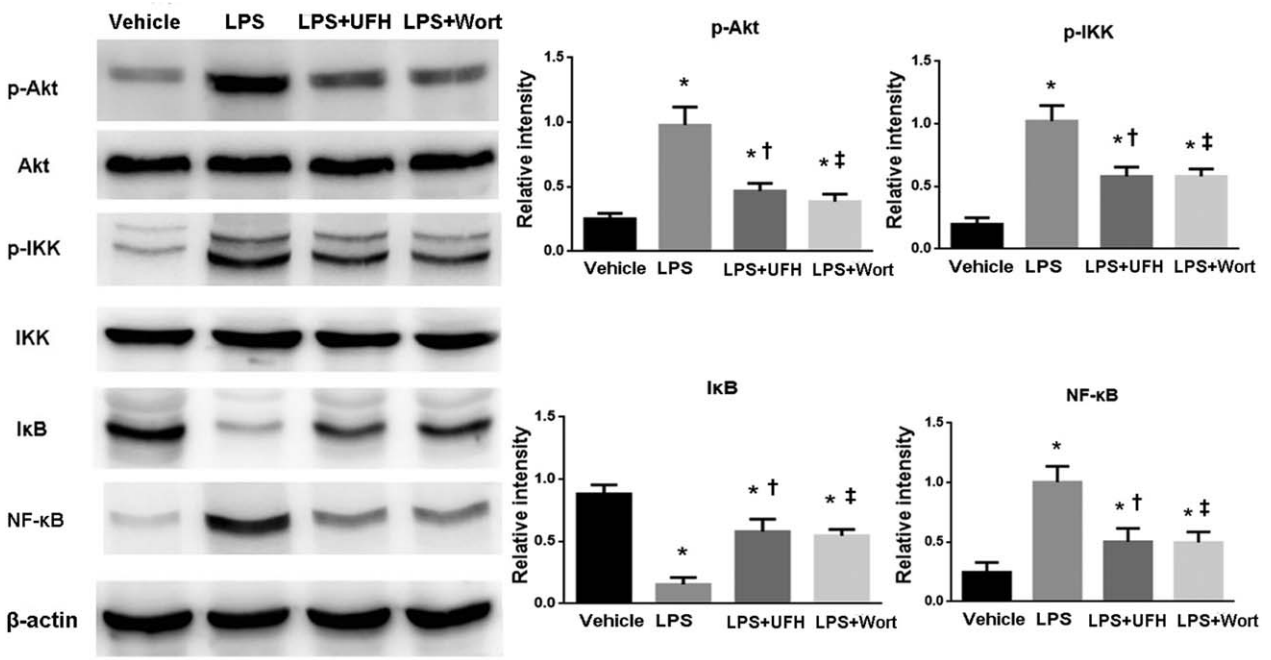

Figure 4: Effect of UFH pre-treatment on the LPS-induced activation of the PI3K/Akt/NF-κB pathway in HPMECs. Cells were pre-treated with UFH (10 U/mL) or wortmannin (100 nmol/L) for 30 min, and then exposed to LPS (10 μg/mL) for 6 h. (A) The expression of p-Akt, Akt, p-IKK, IKK, and IκB was detected by Western blot analysis. (B) The intra-nuclear expression of NF-kB was detected by Western blot analysis. Data are representative of three independent experiments. $^{*}P < 0.05$, compared with the vehicle group. $^{\dagger}P < 0.05$, compared with the LPS-treated group. Akt: Serine/threonine kinase; HPMECs: Human pulmonary microvascular endothelial cells; IKK: IκB kinase; LPS: Lipopolysaccharide; NF-κB: Nuclear factor kappa B; PI3K: Phosphatidylinositol-3 kinase; UFH: Unfractionated heparin; Wort: Wortmannin.

Effects of UFH on LPS-induced PI3K/Akt/NF-κB activation in HPMECs

To assess the effects of UFH on the LPS-induced activation of the PI3K/Akt/NF-κB pathway, Western blot analysis was conducted. As expected, LPS-stimulation increased the expression of p-Akt, p-IKK, and NF-κB in HPMECs. Conversely, UFH or wortmannin (100 nmol/L) clearly inhibited the expression of p-Akt (LPS *vs.* LPS + UFH: 0.977 ± 0.081 *vs.* 0.466 ± 0.035, $P = 0.0045$; LPS *vs.* LPS + Wort [wortmannin]: 0.977 ± 0.081 *vs.* 0.385 ± 0.033, $P = 0.0025$), p-IKK (LPS *vs.* LPS + UFH: 1.023 ± 0.070 *vs.* 0.578 ± 0.044, $P = 0.0060$; LPS *vs.* LPS + Wort: 1.023 ± 0.071 *vs.* 0.580 ± 0.035, $P = 0.0049$), and NF-κB (LPS *vs.* LPS + UFH: 1.003 ± 0.077 *vs.* 0.503 ± 0.065, $P = 0.0078$; LPS *vs.* LPS + Wort: 1.003 ± 0.077 *vs.* 0.497 ± 0.051, $P = 0.0055$), and increased the expression of IκB (LPS *vs.* LPS + UFH: 0.154 ± 0.033 *vs.* 0.580 ± 0.058, $P = 0.0031$; LPS *vs.* LPS + Wort: 0.153 ± 0.032 *vs.* 0.546 ± 0.029, $P = 0.0009$) [Figure 4]. This suggests that PI3K/Akt signaling participates in the LPS-induced activation of the IKK/IκB/NF-κB pathway, and the UFH-mediated protection of the endothelial barrier function against LPS in HPMECs is associated with the PI3K/Akt/NF-κB signaling.

PI3K/Akt/NF-κB signaling contributes to the protective effect of UFH against LPS-induced hyperpermeability of HPMECs

We further studied whether inhibiting PI3K/Akt/NF-κB signaling was associated with the UFH-mediated improvement of LPS-induced hyperpermeability. Indeed, both UFH and wortmannin increased the TEER (LPS *vs.* LPS + UFH: 8.89 ± 0.67 *vs.* 17.72 ± 1.12 $\Omega \cdot cm^2$, $P = 0.0025$; LPS *vs.* LPS + Wort: 8.89 ± 0.67 *vs.* 16.94 ± 1.12 $\Omega \cdot cm^2$, $P = 0.0035$) and decreased FITC-conjugated dextran leakage (LPS *vs.* LPS + UFH: 56.21 ± 2.28 *vs.* 40.54 ± 1.53, $P = 0.0047$; LPS *vs.* LPS + Wort: 56.21 ± 2.28 *vs.* 37.62 ± 1.99, $P = 0.0036$), indicating that UFH protected endothelial cells from LPS-induced hyperpermeability [Figure 5A and 5B].

UFH-mediated inhibition of the LPS-induced decrease in membrane expression of VE-cadherin and p120-catenin, increase in p-MLC expression, and F-actin remodeling is related to PI3K/Akt/NF-κB signaling

As shown in Figure 6A and 6C, UFH and wortmannin protected against the LPS-induced decrease in membrane expression of VE-cadherin (LPS *vs.* LPS + UFH: 0.306 ± 0.049 *vs.* 0.677 ± 0.081, $P = 0.0179$; LPS + Wort: 0.306 ± 0.049 *vs.* 0.602 ± 0.063, $P = 0.0211$) and p120-catenin (LPS *vs.* LPS + UFH: 0.271 ± 0.044 *vs.* 0.776 ± 0.054, $P = 0.0019$; LPS + Wort: 0.271 ± 0.043 *vs.* 0.715 ± 0.092, $P = 0.0122$), and prevented LPS-induced actin remodeling and paracellular gap formation (LPS *vs.* LPS + UFH: 0.973 ± 0.083 *vs.* 0.431 ± 0.049, $P = 0.005$; LPS + Wort: 0.973 ± 0.083 *vs.* 0.492 ± 0.046, $P = 0.0073$), as indicated by immunofluorescence staining [Figure 6A and 6B]. Additionally, UFH and wortmannin inhibited the increase of p-MLC expression (LPS *vs.* LPS + UFH: 0.979 ± 0.086 *vs.* 0.607 ± 0.049, $P = 0.0204$; LPS + Wort: 0.979 ± 0.086 *vs.* 0.523 ± 0.041, $P = 0.0091$) induced by LPS [Figure 6D]. Our results suggest that

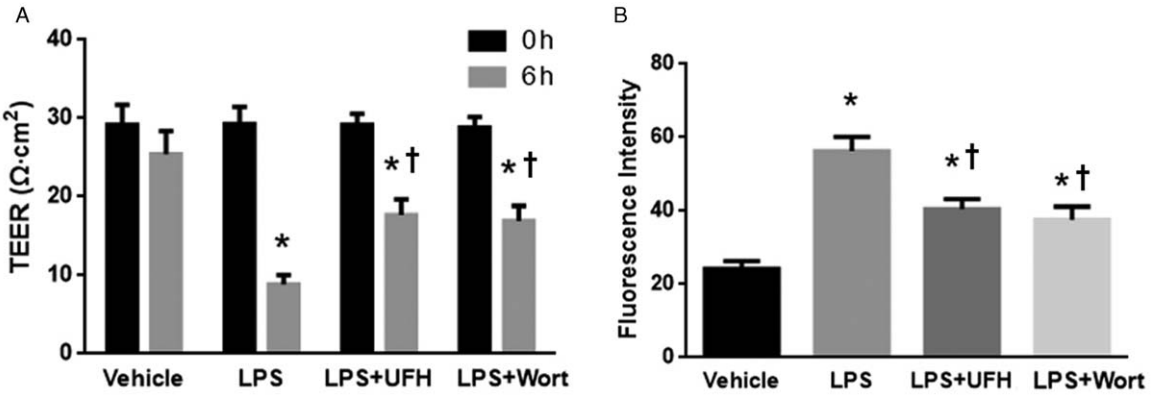

Figure 5: Effect of pre-treatment with UFH or the PI3K/Akt inhibitor wortmannin on the LPS-induced increase in endothelial cell permeability. HPMECs were pre-treated with UFH (10 U/mL) or wortmannin (100 nmol/L) for 30 min, followed by LPS (10 μg/mL) stimulation for 6 h. (A) The TEER across the cells was measured. (B) The influx of fluorescein isothiocyanate-conjugated dextran across the cells was measured. Data are representative of three independent experiments. $^{*}P < 0.05$, compared with the vehicle group, $^{\dagger}P < 0.05$, compared with the LPS-treated group. Akt: Serine/threonine kinase; LPS: Lipopolysaccharide; PI3K: Phosphatidylinositol-3 kinase; TEER: Transendothelial electrical resistance; UFH: Unfractionated heparin; Wort: Wortmannin.

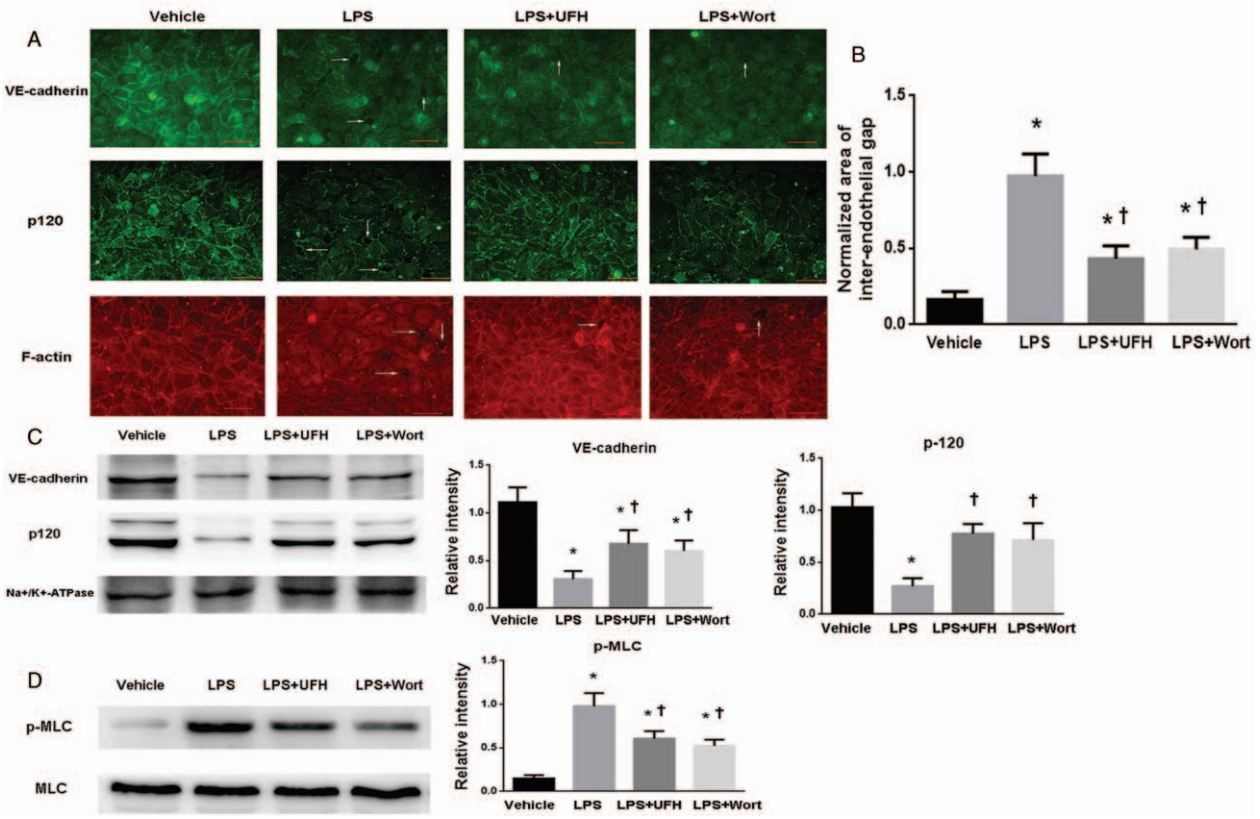

Figure 6: Effect of pre-treatment with UFH or the PI3K/Akt inhibitor wortmannin on the LPS-induced decrease in VE-cadherin membrane localization and F-actin remodeling in HPMECs. (A) Immunofluorescence staining for VE-cadherin and p120-catenin, and tetramethylrhodamine isothiocyanate-phalloidin staining for F-actin. Arrows indicate intercellular gaps. Scale bar = 50 μm. (B) Area of inter-endothelial gaps. The gap area in the field of view was assessed and normalized to the gap area induced with LPS alone. For each group, a total of nine fields of view from three parallel experiments were analyzed. Arrows indicate intercellular gaps. (C) Western blot analysis was used to evaluate the membrane expression of VE-cadherin and p120-catenin. Equal protein loading was confirmed by the Na^{+}/K^{+}-ATPase signal. (D) Western blot analysis was used to evaluate p-MLC expression. Equal protein loading was confirmed by the total MLC signal. Data are representative of three independent experiments. $^{*}P < 0.05$, compared with the vehicle group, $^{\dagger}P < 0.05$, compared with the LPS-treated group. Akt: Serine/threonine kinase; LPS: Lipopolysaccharide; MLC: Myosin light chain; PI3K: Phosphatidylinositol-3 kinase; UFH: Unfractionated heparin; VE-cadherin: Vascular endothelial-cadherin; Wort: Wortmannin.

inhibition of PI3K/Akt/NF-κB signaling might be involved in the UFH-mediated amelioration of LPS-induced inflammation and endothelial barrier dysfunction through VE-cadherin stabilization, decreased phosphorylation of MLC, and reorganization of the actin cytoskeleton.

Discussion

In this study, it was shown that UFH attenuates the LPS-induced dysfunction of the microvascular endothelial barrier by preventing VE-cadherin internalization *in vitro*

and *in vivo*, which may be related with its ability to inhibit the PI3K/Akt/NF-κB pathway in ALI.

It is now widely accepted that malfunctions in the pulmonary endothelial barrier play a vital part in the pathogenesis of ALI. The dynamic regulation of pulmonary vascular endothelial permeability is mainly governed by VE-cadherin-based adherens junctions. The stability of VE-cadherin at the plasma membrane contributes to the regulation of cell adhesion and endothelial barrier function. Decreased membrane expression or internalization of VE-cadherin contributes to endothelial hyperpermeability.[3,4] It has been shown that the interaction of p120-catenin with the juxtamembrane domain of VE-cadherin is the key to controlling the transport of VE-cadherin and its stabilization in the plasma membrane.[25] The loss of VE-cadherin attachment to the actin cytoskeleton and the decrease of VE-cadherin levels due to loss of p120 binding have been related to the regulation of the endothelial barrier function.[11,26] Our results indicate that LPS treatment decreased the membrane expression of VE-cadherin and p120-catenin, as well as F-actin remodeling, both *in vitro* and *in vivo*, leading to pulmonary endothelial hyperpermeability in ALI.

UFH, besides its anti-coagulation effect, exhibits anti-inflammatory effects and prevents LPS- or inflammation-induced endothelial barrier dysfunction.[13-15,23] However, the precise mechanism remains unclear. Previous *in vitro* and *in vivo* studies showed that UFH or low-molecular-weight heparin attenuated the production of inflammatory mediators induced by LPS.[27,28] In this study, UFH inhibited LPS-induced TNF-α production in the BALF of ALI models. Inflammatory cytokines, such as TNF-α, increase vascular endothelial permeability through the formation of intracellular gaps. It was reported that TNF-α treatment enhanced endothelial permeability by increasing the phosphorylation of VE-cadherin or inducing the association between PTK6 and p120-catenin at endothelial cell-cell junctions, causing VE-cadherin internalization.[29,30] Overexpression of p120-catenin in human umbilical vein endothelial cells leads to the stabilization of VE-cadherin surface expression, prevention of VE-cadherin phosphorylation, and inhibition of leukocyte transendothelial migration.[31] Our research suggests that in TNF-α-stimulated HPMECs, the endothelial barrier is disrupted because of a decrease in the membrane localization of VE-cadherin and p120-catenin, consistent with previous studies.[29,30] In addition, p-MLC, a molecule known to orchestrate endothelium remodeling, is required for stress fiber formation associated with endothelial permeability factors.[32,33] Our results show that UFH counteracted the LPS- or TNF-α-induced increase in the expression of p-MLC. These findings indicate that UFH exerts its protective effect on endothelial barrier function by preventing TNF-α-induced changes in the membrane expression of VE-cadherin, p120-catenin, and p-MLC.

PI3K/Akt signaling is involved in endothelial cell mobilization, migration, and homing. The transcription factor NF-κB has a vital part in inflammation because it can induce the transcription of inflammatory mediators. There is evidence suggesting that the PI3K/Akt and NF-κB pathways can inhibit ROS-induced endothelial damage.[16,17,19,20] Studies have shown that LPS or TNF-α induce endothelial cell hyperpermeability via the PI3K/Akt pathway.[34,35] Our previous study showed that the TNF-α-induced increase in iNOS levels in human endothelial cells is mediated by the PI3K-IKK-IκB signaling pathway.[21] UFH was also proved to attenuate LPS-stimulated IL-8 secretion via the PI3K/Akt/NF-κB pathway.[22] In this study, we demonstrated that UFH as well as a PI3K/Akt inhibitor could inhibit the LPS-induced expression of p-Akt and p-IKK, along with NF-κB nuclear translocation. However, a recent study suggests that the effects of LPS on the pulmonary microvascular endothelial barrier function via the PI3K/Akt signaling pathway are concentration dependent.[36] Thus, the lack of experiments using LPS concentration gradients is one weakness of our study. In addition, our study lacks experiments aiming at interfering with the PI3K/Akt signaling to confirm our conclusions. These drawbacks will be addressed in a future study.

Increased vascular permeability is a hallmark of ALI. VE-cadherin has a particularly crucial role in regulating pulmonary endothelial permeability. Thus, enhancing VE-cadherin expression in the pulmonary vasculature could have therapeutic value for ALI. UFH may prove useful in this role and maybe a potential therapeutic agent against ALI.

In conclusion, our study suggests that UFH has a protective effect on the endothelial barrier function in ALI by stabilizing VE-cadherin, which might be mediated by the PI3K/Akt/NF-κB signaling pathway.

Funding

This work was supported by a grant from the Shenyang Science and Technology Plan Project (No. 17-230-9-79).

Conflicts of interest

None.

References

1. Dushianthan A, Grocott MP, Postle AD, Cusack R. Acute respiratory distress syndrome and acute lung injury. Postgrad Med J 2011;87:612–622. doi: 10.1136/pgmj.2011.118398.
2. Johnson ER, Matthay MA. Acute lung injury: epidemiology, pathogenesis, and treatment. J Aerosol Med Pulm Drug Deliv 2010;23:243–252. doi: 10.1089/jamp.2009.0775.
3. Gavard J. Endothelial permeability and VE-cadherin: a wacky comradeship. Cell Adh Migr 2014;8:158–164. doi: 10.4161/cam.29026.
4. Rho SS, Ando K, Fukuhara S. Dynamic regulation of vascular permeability by vascular endothelial cadherin-mediated endothelial cell-cell junctions. J Nippon Med Sch 2017;84:148–159. doi: 10.1272/jnms.84.148.
5. Corada M, Mariotti M, Thurston G, Smith K, Kunkel R, Brockhaus M, *et al*. Vascular endothelial-cadherin is an important determinant of microvascular integrity in vivo. Proc Natl Acad Sci U S A 1999;96:9815–9820. doi:10.1073/pnas.96.17.9815.
6. Fu P, Usatyuk PV, Lele A, Harijith A, Gregorio CC, Garcia JG, *et al*. c-Abl mediated tyrosine phosphorylation of paxillin regulates LPS-induced endothelial dysfunction and lung injury. Am J Physiol Lung Cell Mol Physiol 2015;308:L1025–L1038. doi: 10.1152/ajplung.00306.2014.

7. Huang Y, Tan Q, Chen R, Cao B, Li W. Sevoflurane prevents lipopolysaccharide-induced barrier dysfunction in human lung microvascular endothelial cells: Rho-mediated alterations of VE-cadherin. Biochem Biophys Res Commun 2015;468:119–124. doi: 10.1016/j.bbrc.2015.10.150.
8. Schulte D, Kuppers V, Dartsch N, Broermann A, Li H, Zarbock A, *et al*. Stabilizing the VE-cadherin-catenin complex blocks leukocyte extravasation and vascular permeability. EMBO J 2011;30:4157–4170. doi: 10.1038/emboj.2011.304.
9. Ishiyama N, Lee SH, Liu S, Li GY, Smith MJ, Reichardt LF, *et al*. Dynamic and static interactions between p120 catenin and E-cadherin regulate the stability of cell-cell adhesion. Cell 2010;141:117–128. doi: 10.1016/j.cell.2010.01.017.
10. Iyer S, Ferreri DM, DeCocco NC, Minnear FL, Vincent PA. VE-cadherin-p120 interaction is required for maintenance of endothelial barrier function. Am J Physiol Lung Cell Mol Physiol 2004;286:L1143–L1153. doi: 10.1152/ajplung.00305.2003.
11. Xiao K, Allison DF, Buckley KM, Kottke MD, Vincent PA, Faundez V, *et al*. Cellular levels of p120 catenin function as a set point for cadherin expression levels in microvascular endothelial cells. J Cell Biol 2003;163:535–545. doi: 10.1083/jcb.200306001.
12. Vignoli A, Marchetti M, Balducci D, Barbui T, Falanga A. Differential effect of the low-molecular-weight heparin, dalteparin, and unfractionated heparin on microvascular endothelial cell hemostatic properties. Haematologica 2006;91:207–214.
13. Han J, Ding R, Zhao D, Zhang Z, Ma X. Unfractionated heparin attenuates lung vascular leak in a mouse model of sepsis: role of RhoA/Rho kinase pathway. Thromb Res 2013;132:e42–e47. doi: 10.1016/j.thromres.2013.03.010.
14. Li X, Zheng Z, Mao Y, Ma X. Unfractionated heparin promotes LPS-induced endothelial barrier dysfunction: a preliminary study on the roles of angiopoietin/Tie2 axis. Thromb Res 2012;129:e223–e228. doi: 10.1016/j.thromres.2012.03.003.
15. Mu S, Liu Y, Jiang J, Ding R, Li X, Li X, *et al*. Unfractionated heparin ameliorates pulmonary microvascular endothelial barrier dysfunction via microtubule stabilization in acute lung injury. Respir Res 2018;19:220. doi: 10.1186/s12931-018-0925-6.
16. Ahmad KA, Ze H, Chen J, Khan FU, Xuezhuo C, Xu J, *et al*. The protective effects of a novel synthetic beta-elemene derivative on human umbilical vein endothelial cells against oxidative stress-induced injury: involvement of antioxidation and PI3k/Akt/eNOS/NO signaling pathways. Biomed Pharmacother 2018;106:1734–1741. doi: 10.1016/j.biopha.2018.07.107.
17. Chu P, Han G, Ahsan A, Sun Z, Liu S, Zhang Z, *et al*. Phosphocreatine protects endothelial cells from methylglyoxal induced oxidative stress and apoptosis via the regulation of PI3K/Akt/eNOS and NF-kappaB pathway. Vascul Pharmacol 2017;91:26–35. doi: 10.1016/j.vph.2016.08.012.
18. Zhou B, Weng G, Huang Z, Liu T, Dai F. Arctiin prevents LPS-induced acute lung injury via inhibition of PI3K/AKT signaling pathway in mice. Inflammation 2018;41:2129–2135. doi: 10.1007/s10753-018-0856-x.
19. Jiang K, Guo S, Yang C, Yang J, Chen Y, Shaukat A, *et al*. Barbaloin protects against lipopolysaccharide (LPS)-induced acute lung injury by inhibiting the ROS-mediated PI3K/AKT/NF-kappaB pathway. Int Immunopharmacol 2018;64:140–150. doi: 10.1016/j.intimp.2018.08.023.
20. Qi S, Xin Y, Guo Y, Diao Y, Kou X, Luo L, *et al*. Ampelopsin reduces endotoxic inflammation via repressing ROS-mediated activation of PI3K/Akt/NF-kappaB signaling pathways. Int Immunopharmacol 2012;12:278–287. doi: 10.1016/j.intimp.2011.12.001.
21. Zheng Z, Li Z, Chen S, Pan J, Ma X. Tetramethylpyrazine attenuates TNF-alpha-induced iNOS expression in human endothelial cells: involvement of Syk-mediated activation of PI3K-IKK-IkappaB signaling pathways. Exp Cell Res 2013;319:2145–2151. doi: 10.1016/j.yexcr.2013.05.018.
22. Li X, Liu Y, Wang L, Li Z, Ma X. Unfractionated heparin attenuates LPS-induced IL-8 secretion via PI3K/Akt/NF-kappaB signaling pathway in human endothelial cells. Immunobiology 2015;220:399–405. doi: 10.1016/j.imbio.2014.10.008.
23. Ding R, Zhao D, Guo R, Zhang Z, Ma X. Treatment with unfractionated heparin attenuates coagulation and inflammation in endotoxemic mice. Thromb Res 2011;128:e160–e165. doi: 10.1016/j.thromres.2011.07.044.
24. Monaghan-Benson E, Wittchen ES. In vitro analyses of endothelial cell permeability. Methods Mol Biol 2011;763:281–290. doi: 10.1007/978-1-61779-191-8_19.
25. Kourtidis A, Ngok SP, Anastasiadis PZ. p120 catenin: an essential regulator of cadherin stability, adhesion-induced signaling, and cancer progression. Prog Mol Biol Transl Sci 2013;116:409–432. doi: 10.1016/B978-0-12-394311-8.00018-2.
26. Garrett JP, Lowery AM, Adam AP, Kowalczyk AP, Vincent PA. Regulation of endothelial barrier function by p120-cateninVE-cadherin interaction. Mol Biol Cell 2017;28:85–97. doi: 10.1091/mbc.E16-08-0616.
27. Li X, Zheng Z, Li X, Ma X. Unfractionated heparin inhibits lipopolysaccharide-induced inflammatory response through blocking p38 MAPK and NF-kappaB activation on endothelial cell. Cytokine 2012;60:114–121. doi: 10.1016/j.cyto.2012.06.008.
28. Luan ZG, Naranpurev M, Ma XC. Treatment of low molecular weight heparin inhibits systemic inflammation and prevents endotoxin-induced acute lung injury in rats. Inflammation 2014;37:924–932. doi: 10.1007/s10753-014-9812-6.
29. Angelini DJ, Hyun SW, Grigoryev DN, Garg P, Gong P, Singh IS, *et al*. TNF-alpha increases tyrosine phosphorylation of vascular endothelial cadherin and opens the paracellular pathway through fyn activation in human lung endothelia. Am J Physiol Lung Cell Mol Physiol 2006;291:L1232–L1245. doi: 10.1152/ajplung.00109.2006.
30. Haines RJ, Beard RS Jr, Wu MH. Protein tyrosine kinase 6 mediates TNFalpha-induced endothelial barrier dysfunction. Biochem Biophys Res Commun 2015;456:190–196. doi: 10.1016/j.bbrc.2014.11.057.
31. Alcaide P, Martinelli R, Newton G, Williams MR, Adam A, Vincent PA, *et al*. p120-Catenin prevents neutrophil transmigration independently of RhoA inhibition by impairing Src dependent VE-cadherin phosphorylation. Am J Physiol Cell Physiol 2012;303:C385–C395. doi: 10.1152/ajpcell.00126.2012.
32. Gilbert-McClain LI, Verin AD, Shi S, Irwin RP, Garcia JG. Regulation of endothelial cell myosin light chain phosphorylation and permeability by vanadate. J Cell Biochem 1998;70:141–155. doi: 10.1002/(SICI)1097-4644(19980701)70:1%3C141::AID-JCB14%3E3.0.CO;2-S.
33. Recoquillon S, Carusio N, Lagrue-Lakhal AH, Tual-Chalot S, Filippelli A, Andriantsitohaina R, *et al*. Interaction in endothelium of non-muscular myosin light-chain kinase and the NF-kappaB pathway is critical to lipopolysaccharide-induced vascular hyporeactivity. Clin Sci (Lond) 2015;129:687–698. doi: 10.1042/cs20140625.
34. Xu H, Song J, Gao X, Xu Z, Xu X, Xia Y, *et al*. Paeoniflorin attenuates lipopolysaccharide-induced permeability of endothelial cells: involvements of F-actin expression and phosphorylations of PI3K/Akt and PKC. Inflammation 2013;36:216–225. doi: 10.1007/s10753-012-9537-3.
35. Zhang Y, Han Y, Zhao Y, Lv Y, Hu Y, Tan Y, *et al*. DT-13 ameliorates TNF-alpha-induced vascular endothelial hyperpermeability via non-muscle myosin IIA and the Src/PI3K/Akt signaling pathway. Front Immunol 2017;8:925. doi: 10.3389/fimmu.2017.00925.
36. Zheng X, Zhang W, Hu X. Different concentrations of lipopolysaccharide regulate barrier function through the PI3K/Akt signalling pathway in human pulmonary microvascular endothelial cells. Sci Rep 2018;8:9963. doi: 10.1038/s41598-018-28089-3.

How to cite this article: Mu ST, Tang J, Ma JQ, Zhong Y, Liu HZ, Ma XC, Zheng Z. Unfractionated heparin attenuates endothelial barrier dysfunction via the phosphatidylinositol-3 kinase/serine/threonine kinase/nuclear factor kappa-B pathway. Chin Med J 2020;133:1815–1823. doi: 10.1097/CM9.0000000000000905